The EMBO Journal Vol.16 No.16 pp.4817–4825, 1997

Random mutagenesis reveals a region important for gating of the yeast K^+ channel Ykc1

Stephen H.Loukin[1], Brian Vaillant[1], Xin-Liang Zhou[1], Edgar P.Spalding[2], Ching Kung[1,3] and Yoshiro Saimi[1,4]

[1]Laboratory of Molecular Biology and Departments of [2]Botany and [3]Genetics, University of Wisconsin, Madison, WI 53706, USA

[4]Corresponding author

***YKC1* (*TOK1*, *DUK1*, *YORK*) encodes the outwardly rectifying K^+ channel of the yeast plasma membrane. Non-targeted mutations of *YKC1* were isolated by their ability to completely block proliferation when expressed in yeast. All such mutations examined occurred near the cytoplasmic ends of the transmembrane segments following either of the duplicated P loops, which we termed the 'post-P loop' (PP) regions. These PP mutations specifically caused marked defects in the 'C_1' states, a set of interrelated closed states that Ykc1 enters and exits at rates of tens to hundreds of milliseconds. These results indicate that the Ykc1 PP region plays a role in determining closed state conformations and that non-targeted mutagenesis and microbial selection can be a valuable tool for probing structure–function relationships of ion channels.**

Keywords: gating/K^+ channel/*TOK1*/yeast/*YKC1*

Introduction

Patch–clamp recordings of the *Saccharomyces cerevisiae* plasma membrane reveal an outwardly rectifying K^+ current (Gustin *et al.*, 1986; Bertl *et al.*, 1993), a stretch activated current (Gustin *et al.*, 1988) and a less prominent inward K^+ current conducted through a K^+ transporter (Bertl *et al.*, 1995). The gene encoding the outwardly rectifying K^+ channel, *YKC1* (also known as *TOK1*, *DUK1* and *YORK*), was identified from the yeast genomic sequence (Miosga *et al.*, 1994) by virtue of its conserved P regions (Ketchum *et al.*, 1995; Zhou *et al.*, 1995; Lesage *et al.*, 1996; Reid *et al.*, 1996). Deletion of *YKC1* results in complete elimination of the outwardly rectifying plasma membrane K^+ current (Zhou *et al.*, 1995; Reid *et al.*, 1996).

Ykc1 has two P regions embedded in a predicted topology of M1-M2-M3-M4-M5-P1-M6-M7-P2-M8. The first M1–M6 topology is reminiscent of many voltage- or cyclic nucleotide-gated (V or CNG) channels, including K^+, Na^+, Ca^{2+} and non-selective cation channels. The second P region appears to have arisen by a tandem duplication of the P1 region (Reid *et al.*, 1996). Interestingly, there are now several 'two pored' channels found to have an M1-P1-M2-M3-P2-M4 motif (Fink *et al.*, 1996; Goldstein *et al.*, 1996; Czempinski *et al.*, 1997; Lesage *et al.*, 1997). The P regions of Ykc1 are more similar to the 6-transmembrane K^+ channels than to the IRK-type 2-transmembrane K^+ channels (Zhou *et al.*, 1995). Outside its P regions Ykc1 shares little primary sequence homology with other channels.

When expressed in oocytes, *YKC1* produces a K^+-selective, outwardly rectifying current with properties similar to those of natively expressed *YKC1*. These properties include a high degree of K^+ selectivity, strong outward rectification and a characteristic flickery open channel behavior. There is disagreement as to whether the outward rectification of *YKC1* is a function of the electrochemical driving force for K^+ ($\Delta\mu_{K+}$) (Ketchum *et al.*, 1995; Lesage *et al.*, 1996) or the absolute membrane voltage (V_m) (Zhou *et al.*, 1995; Reid *et al.*, 1996). We agree with Ketcham *et al.* (1995) and Lesage *et al.* (1996) that the rectification of oocyte-expressed *YKC1* is primarily determined by $\Delta\mu_{K+}$ (Loukin *et al.*, in preparation). It was originally reported that the rectification of Ykc1 was due to a blockage by external cations (Ketchum *et al.*, 1995), but other investigators have failed to confirm such a divalent ion dependence of Ykc1 rectification (Zhou *et al.*, 1995; Lesage *et al.*, 1996). Activation of Ykc1 is modeled as a

$$C_1 \leftrightarrow C_2 \leftrightarrow O$$

transition (Lesage *et al.*, 1996), where C_2 is an instantaneously activating state and C_1 is slowly activating states.

In this report we describe the novel application of non-targeted mutagenesis and classical microbial selection towards a structure–function study of *YKC1*. Mutations of functional consequence were isolated from randomly mutagenized alleles of *YKC1* by their ability to block growth. These alleles were expected to result from loss of regulatory function, such as gating or ionic filtration, since deletion of *YKC1* does not affect proliferation under standard conditions. The advantage of this non-targeted strategy over standard targeted mutagenesis is that it does not require nor make *a priori* assumptions about either the physiological relevance of channel functions or the location of the mutational target. These mutants have furthered our understanding of C_1 and C_2. In the light of localizations of the gating function in V and CNG channels (Gordon and Zagotta, 1995), our results appear to indicate that the PP region may be part of a conserved gating structure of V and CNG channels.

Results

Isolation of YKC1 mutations that block growth

As reported previously (Zhou *et al.*, 1995; Reid *et al.*, 1996), deletion of *YKC1* eliminates the outward rectifying K^+ current of the yeast plasma membrane. Ykc1 channel activity can be restored in such deletion strains by expressing *YKC1* from plasmid pGALYKC1, which contains the *YKC1* open reading frame (ORF) inserted down-

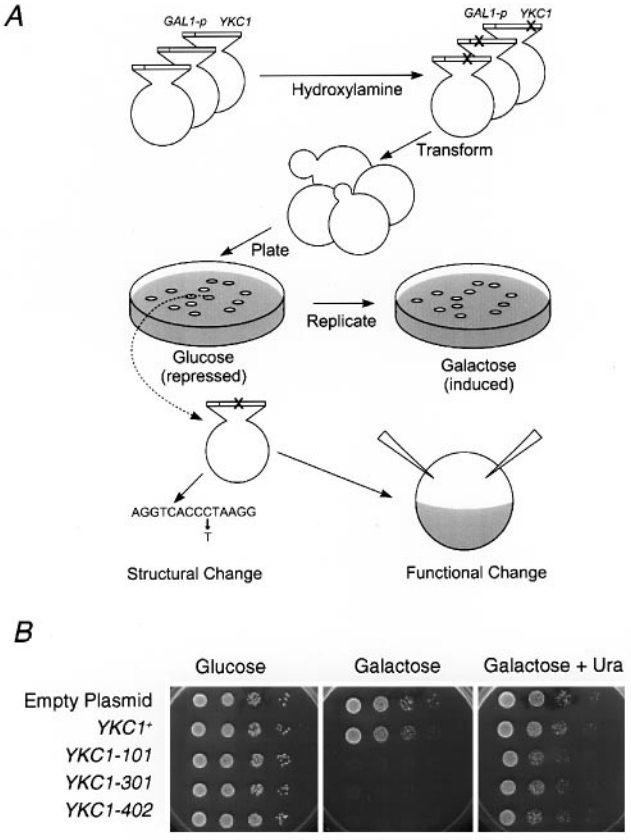

Fig. 1. Isolation of *YKC1* mutant alleles that block yeast proliferation. (**A**) Summary of the screen used to isolate *YKC1* mutants of functional consequence. See Material and methods for a detailed description. (**B**) Growth blocking phenotype of *YKC1* mutants. Equal titers of cells of yeast strain αku8 transformed with the empty plasmid pGALURA, wild-type *YKC1*-expressing pGALYKC1 (*YKC1*$^+$) or mutant *YKC1*-expressing pGALYKC-X (where X is the corresponding mutant allele number) were serially 10-fold diluted (left to right) and allowed to form colonies under conditions which: repressed *YKC1* expression (glucose); induced expression of *YKC1* (galactose); induced expression of *YKC1* but allowed cells which had spontaneously lost their plasmids to proliferate (galactose + uracil). As can be seen, the mutant *YKC1* caused galactose sensitivity, which was a plasmid-dependent phenotype since it occurred only when cells were concomitantly required to maintain their plasmids.

stream of the galactose-inducible *GAL1* promoter. No Ykc1 current could be detected in the plasma membrane of a *YKC1* deletion yeast strain (αku8) alone nor in this strain bearing plasmid pGALYKC1 (αku8[pGALYKC1]) cultured in glucose. Ykc1 current increases to levels several fold higher than its native expression when this strain is cultured in the presence of galactose.

To screen for *YKC1* mutations which cause deleterious channel activities, four pools of pGALYKC1 plasmids were mutagenized with hydroxylamine (HA) and transformed separately into αku8 yeast cells (Figure 1A) (note that HA, though commonly used, primarily induces CG→TA transitions and this limits the range of mutations available; see Discussion). Such a strategy guarantees that mutant plasmids isolated from separate pools have resulted from independent mutagenic events. Note that the plasmids and not the yeast cells were mutagenized *in vitro* and the chromosomal copy of *YKC1* in αku8 had been deleted. These transformed cells were plated onto synthetic glucose medium (SD) lacking uracil (Sherman, 1991), which selected for the presence of the plasmid while repressing mutagenized *YKC1*. The resultant colonies were replica plated onto a similar medium with glucose replaced by galactose (SG), which induced expression of mutagenized *YKC1* in plasmids. Replica that failed to grow on the SG plate were isolated from the SD plate. These galactose-sensitive strains were further plated onto SG containing uracil to test whether the cells which spontaneously lost their plasmids and hence the mutated *YKC1* gene (~1% per division under non-selective conditions; Ausubel *et al.*, 1993) could grow. Figure 1B (right) shows that the galactose-sensitive phenotype was indeed plasmid encoded.

From ~40 000 colonies screened, 14 were isolated containing plasmids that stop growth in galactose (Figure 1B, three mutants shown). Those causing slower growth were not included in this report. The plasmids were recovered from these strains and these *YKC1* alleles were named *YKC1*-xxx where the first x indicates which of the four mutagenized plasmid pools they came from to delineate mutational independence. The *YKC1* ORFs from two of these plasmids were also subcloned into identical but unmutagenized vectors from which they also conferred the galactose-sensitive phenotype to transformed yeast, verifying that this phenotype was caused by mutations in the *YKC1* ORFs and not those occurring elsewhere in the plasmid. Six of these 14 alleles were chosen at random from the four pools for further analysis.

Growth blocking mutations all occurred at the cytoplasmic ends of the post-P loop membrane spanning domains

The DNA sequences of these six mutant alleles were determined. Two independent isolates, *YKC1*-301 and *YKC1*-401, both contain a T322I substitution, *YKC1*-201, *YKC1*-304 and *YKC1*-402 contain a S330F substitution and *YKC1*-101 contains a V456I substitution (Figure 2A). *YKC1*-201 and *YKC1*-401 contain additional silent I248I and F409F nucleotide mutations. The repeated T322I and S330F alleles arose from independent mutagenic events, since they were isolated from separately mutagenized plasmid pools, indicating that at most only a few other hydroxylamine-mutable sites would elicit such a phenotype. The clustering of the mutations is striking, since they all occur at the cytoplasmic ends of the membrane spanning domains following either P loop, M6 or M8, termed the 'PP' (post-P loop) region (Figure 2A). All six mutations occurred within a 10 amino acid window downstream of the aligned P loop, sequences (Figure 2B). Ykc1 comprises 691 residues. Even if the size of this window is doubled to 20 amino acids (solid bordered box in Figure 2B), the chance of six independent mutations randomly appearing in such a window by chance alone is <1 in 1 000 000. Thus, CT→AG transitions that completely block proliferation on SG appear to exclusively occur in the PP regions.

PP mutations do not affect the O or C_2 state

The channel activities of the wild-type and all three mutant alleles, *YKC1*-101 (V456I), *YKC1*-301 (T322I) and *YKC1*-402 (S330F), were analyzed. I–V plots show that the steady-state ensemble currents of both wild-type and the mutants, all of which were well expressed in oocytes,

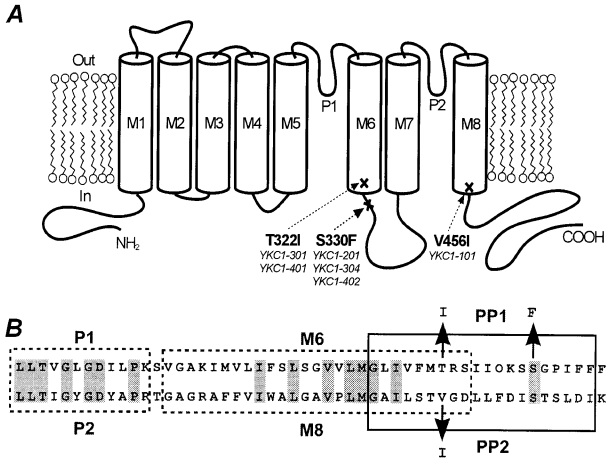

Fig. 2. Location of growth blocking mutations of Ykc1. Both strands of six mutant alleles of *YKC1* which blocked proliferation completely were sequenced. Both strands of all six alleles were sequenced. Non-silent mutations occurred in only three residues. The multiple instances of T322I and S330F were due to independent mutagenic events since they were isolated separately from the original mutagenesis reactions. (**A**) These mutations cluster in a common topological region, the intracellular junction of the membrane spanning domains immediately following either P loop, a region we called 'PP' for post-P loop. (**B**) The P1 M6 and P2 M8 regions are aligned and marked. The PP regions, defined as an area of 20 residues surrounding the growth blocking mutations, are marked with solid edged boxes. Identical residues are shaded. Note that the T322I and the V456I mutations are precisely equidistant from the P loops.

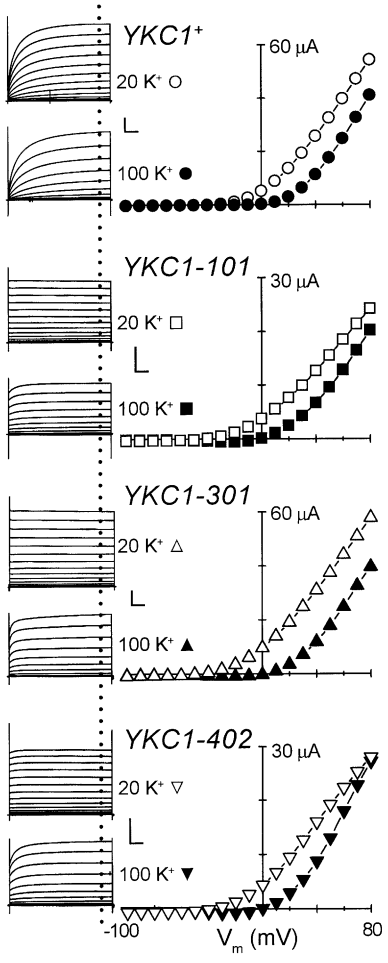

Fig. 3. Wild-type and PP mutant channels maintain steady-state rectification. Whole cell currents were recorded from oocytes injected with RNA transcribed from wild-type and each of the three different mutant alleles of *YKC1*. Near steady-state current was measured 900 ms (dotted line) after stepping from the holding potential of –80 mV to test potentials of between –100 and +80 mV at 10 mV intervals in 20 (open symbols) and 100 mM (closed symbols) bath K^+. The near steady-state rectification is not significantly affected by PP mutations. For both wild-type and the mutants there was no significant inward current and the current activation threshold was near the predicted E_K. Currents were recorded from oocytes 3–5 days after injection with ~50 ng synthetic mRNA. Bath solutions contained 5 mM HEPES, pH 7.5, 1 mM $MgCl_2$, 1 mM $CaCl_2$ and either 100 or 20 mM KCl and 80 mM NaCl. Traces were neither leak subtracted nor compensated for capacitance. All calibration bars 10 μA×100 ms.

rectify outwardly with no substantial inward currents at any potential (Figure 3). Raising external K^+ 5-fold from 20 (open symbols) to 100 mM (closed symbols) causes an ~40 mV rightward shift in the threshold of activation of outward currents in both the wild-type and the mutants, similar to the +40 mV shift this substitution would have on E_K. Thus the steady-state current–voltage relationships, being largely determined by $\Delta\mu_{K+}$, not V_m, are not substantially affected by the PP mutations.

Direct examination of the rapid $C_2 \rightarrow O$ activation (see Introduction) demonstrates that C_2 remains largely intact in the PP mutants. Using recording techniques designed to detect sub-millisecond transitions (see Materials and methods), the time dependence of the 'instantaneous' activation from C_2 can in fact be seen (Figure 4A, top; note that the entire trace is only 1 ms here). This $C_2 \rightarrow O$ activation occurs notably more slowly than the time it takes for V_m to equilibrate to the command potential (Figure 4A, bottom), ruling out that this time dependence is an artifact of the time dependence of charging the oocyte. When the capacitive component of the outward current is subtracted, this activation from C_2 can be seen to have a rate upon depolarization to +80 mV of ~100 μs (Figure 4B). Activation from C_2 of Ykc1-101 (Figure 4C) appears similar to that of the wild-type. Thus, this PP mutation does not significantly affect the rapid transition from C_2 to O.

The PP mutations also had no substantial effect on the outward conducting properties of O. Substitution of cytoplasmic K^+ with either Na^+ or NH_4^+ abolished outward currents in inside-out patches of both *YKC1*$^+$- and *YKC1*-101-expressing oocytes (Figure 5), indicating that Ykc1-101 maintained the wild-type selectivity for K^+. Similar results were obtained with the other two PP mutant types (data not shown). The apparent unitary slope conductance calculated from single channel excised patches was 22.0 ± 1.9 pS for Ykc1-101, similar to the 20.3 ± 2.5 pS for Ykc1$^+$ (mean ± SD, n = 3). Note that these conductances are probably underestimates of the true open channel conductance, due to the flickery open channel behavior of Ykc1 (Bertl *et al.*, 1993).

PP mutations decrease residence in and alter activation from the C_1 states

Fitting the delayed activation from the C_1 states (see Introduction) of the wild-type required three rate constants of 14.9 ± 2.9, 71.8 ± 9.0 and 275 ± 13 ms when depolarized from –80 to +80 mV at 23°C in 100 mM K^+ (n = 6 separate oocytes) (Figure 6A, individual rate components illustrated by dotted traces at the bottom of

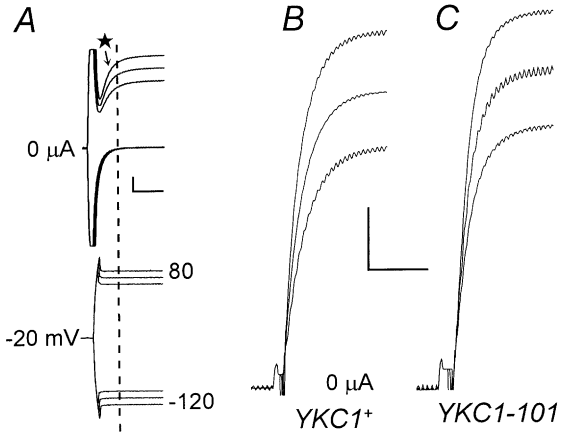

Fig. 4. PP mutation does not affect activation from C_2. Note the rapid time scale displayed, with all the traces in this figure showing only 1 ms or 1/1000 the time course illustrated in the whole cell traces of the previous figures. All calibration bars are 15 μA×0.4 ms. (**A**) (Upper traces) Whole cell currents of oocytes expressing wild-type Ykc1 upon voltage steps from –20 mV to +80, +70, +60, –100, –110 and –120 mV in 100 mM external K^+. The capacitive currents can be seen upon all voltage steps. Rapid activation from the C_2 state can clearly be resolved after these capacitive surges upon depolarization (star). (Lower traces) V_m was simultaneously monitored with the current shown in (A) to verify that V_m in fact reached the command potential before significant $C_2 \rightarrow O$ activation occurred. The vertical dashed line marks the same time point in both the upper and lower traces to help show that the command potential was reached long before the majority of $C_2 \rightarrow O$ activation had occurred. (**B**) Traces showing $C_2 \rightarrow O$ activation with the capacitive currents subtracted by addition of the –120, –110 and –100 mV traces to the +80, +70 and +60 traces respectively in (A). Wild-type Ykc1 was activated from C_2 at a rate of ~100 μs. (**C**) Capacitance-subtracted $C_2 \rightarrow O$ activation of Ykc1-101-expressing oocytes shows that this activation is not affected by this PP mutation. All currents were recorded from oocytes 3 days after injection with ~100 ng *YKC1* RNA to induce high current expression. Electrical recording techniques are described in Materials and methods.

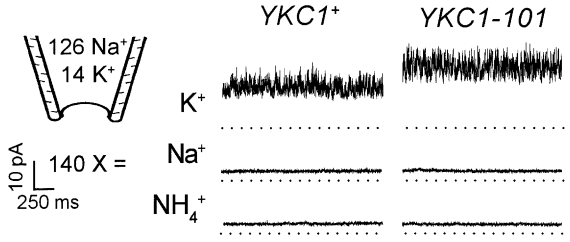

Fig. 5. PP mutant channels maintain ionic selectivity. Ionic selectivities were determined by perfusing bath solutions containing the stated cations over the cytoplasmic face of inside-out patches from oocytes expressing either multiple wild-type or Ykc1-101 channels. Outward currents were observed in both cases only when K^+, but not Na^+ or $NH4^+$, was present on the cytoplasmic side. Currents were recorded at a V_m of +50 mV. The higher current level of the Ykc1-101 trace results from higher expression levels. Bath (cytoplasmic) solutions contained 140 mM chloride salt of the stated cation and 5 mM EGTA. Pipette (external) solutions contained 14 mM KCl, 126 mM NaCl. Both solutions also contained 1 mM $CaCl_2$, 1 mM $MgCl_2$ and 5 mM HEPES, pH 7.2. Dashed lines represent zero current levels. Leakage was not subtracted.

the *YKC1*$^+$ plot). Thus, C_1 is actually a set of closed states. Entry into the C_1 states is favored by negative voltage (Figure 6B). Comparing the distribution of channels in the C_1 states in 100 mM K^+ (Figure 6B, ●) with that in 20 mM K^+ (Figure 6D, ○), it can be seen that high external K^+ also favors residence in C_1. The 31 mV negative shift of the Boltzmann distribution between C_1 and C_2 caused by decreasing external K^+ from 100 to 20 mM is close to the –38 mV shift such a lowering of K^+ would be predicted to have on E_K, suggesting that distribution between C_1 and C_2 is determined, at least in part, by $\Delta\mu_{K+}$ (a further examination of the wild-type C_1–C_2 distribution will be presented in Loukin *et al.*, in preparation).

In contrast to activation from rapidly activating C_2, residence in and activation from the delayed C_1 states were notably affected by the PP mutations. The PP mutations caused a >50 mV negative shift in the holding potential at which Ykc1 starts to significantly dwell in C_1 (Figure 6 B and D). Whereas wild-type Ykc1 exclusively resides in C_1 at –100 mV in 100 mM K^+ (Figure 6B, ●), extrapolation of the Boltzmann fits of C_1 residence versus holding potential showed that <55% of Ykc1-101 and Ykc-402 and <32% of Ykc1-301 channels maximally reside in the delayed C_1 states even at highly negative voltages (Figure 6B). In 20 mM K^+ <32% of Ykc1-101 and Ykc-402 and <10% of Ykc1-301 channels maximally dwell in C_1. Thus at mildly negative potentials, where a significant fraction of wild-type channels are in C_1 (e.g. 0 to –50 mV in 100 mM K^+), almost none of the mutant channels are. At highly negative potentials, the likely yeast resting potential, wild-type Ykc1 channels will exclusively reside in the delayed C_1 states, whereas at most 55% of the mutant channels will, with the remainder residing in rapidly activating C_2.

The remnant of the mutant Ykc1-101 delayed current activation can be fitted to two exponentials of 33.8 ± 11.4 and 111 ± 20 ms when depolarized from –80 to +80 mV in 100 mM K^+ at 23°C (n = 5 separate oocytes, illustrated as dotted lines in Figure 6A, *YKC1*-101). Thus, all three wild-type delayed C_1 states activations were altered by the single V456I mutation, indicating the structural relatedness of the individual C_1 states. That the rapid $C_2 \rightarrow O$ transition was unaffected by this same mutation (Figure 4) in contrast demonstrates the physical distinction between C_2 and C_1.

The mutants lack of delayed activation from the C_1 states is clearly seen at the single channel level as well (Figure 7). Latency analysis on single channel patches demonstrated a lack residence in the delayed C_1 states in the mutant. When patches containing single wild-type Ykc1 channels were depolarized from –80 mV, there was a characteristic lag of tens to hundreds of milliseconds before the channel opened (Figure 7, *). This same degree of latency was not seen when the patch was stepped from +40 mV (Figure 7, top right), demonstrating that this latency was due to a transition from the C_1 states. When stepped from –80 mV, Ykc1–101 channels did not show such a latency (Figure 7, bottom). Thus, activation from the delayed C_1 states in the wild-type, as well as its absence in the PP mutants, can be observed at the single channel level.

Both wild-type and Ykc1-101 single channels rapidly flicker, which may be due to rapid $C_2 \leftrightarrow O$ transitions at positive potentials. Visual inspection discerned little difference in this flicker between wild-type and mutant channels. It is also notable that the mutant channels closed for up to 200 ms at positive potentials, possibly reflecting an inactivating state of Ykc1 unrelated to the C_1 states.

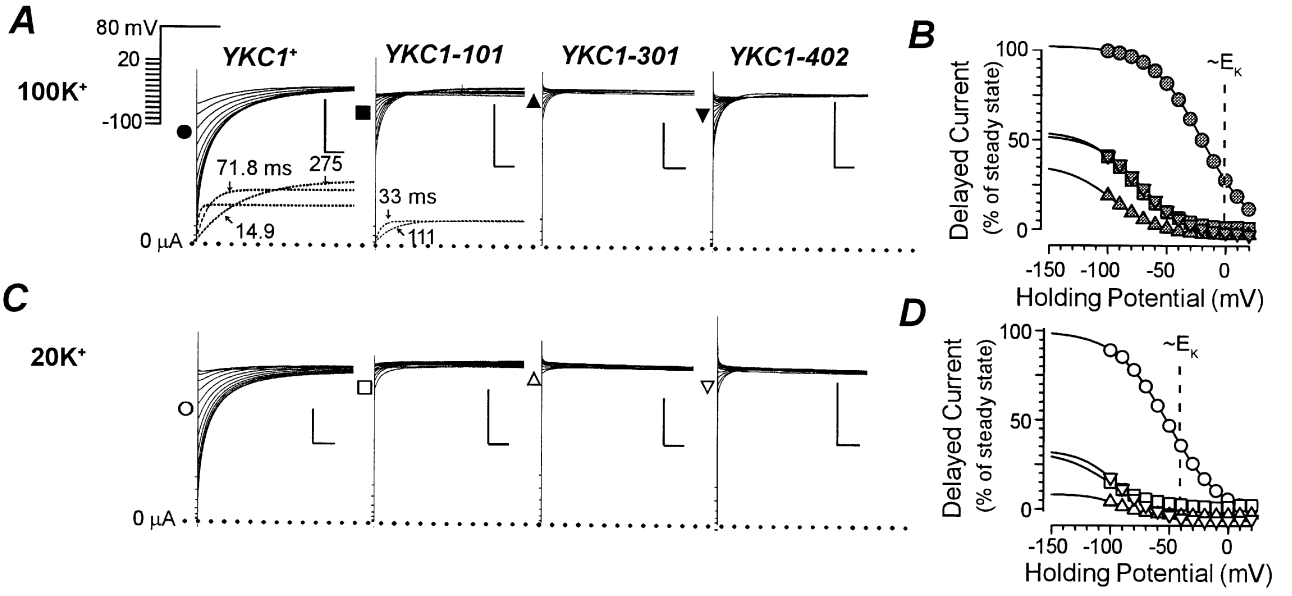

Fig. 6. PP mutations severely affect residence in and activation from the C_1 closed states. (**A**) Current activations upon stepping to +80 mV from holding potentials between –100 and +20 mV at 10 mV intervals were recorded from whole oocytes expressing wild-type (●), Ykc1-101 (■), Ykc1-301 (▲) and Ykc1-402 (▼) in 100 mM bath K^+. Three exponential components were required to adequately fit the current activation from –80 to +80 mV of the $Ykc1^+$ current, whereas only two such components were required for Ykc1-101 current activation (dotted lines show extrapolated contributions from individual activations to scale). Thus delayed activation of Ykc1 occurs from three distinct C_1 states; the single V456I mutation of Ykc1-101 alters all three. (**B**) The fraction of steady-state current which was activated with delayed kinetics is plotted as a function of holding potential. Lines are Boltzmann fits of the raw data (symbols). $V_{1/2}$ (curve midpoint), k (slope factor) and A (maximum amplitude) of the Boltzmann fits were –19.8 mV, 21.5% and 102.3% for wild-type, –79.7 mV, 18.8% and 54.7% for *YKC1*-101, –95.3 mV, 20.1% and 36.3% for *YKC1*-301 and –72.7 mV, 20.1% and 52.8% for *YKC1*-402. Thus, a negative extrapolation of these fits indicates that while wild-type channels reside exclusively in C_1 at sufficiently negative voltages, the maximal extent to which Ykc1-101 and Ykc1-402 dwelt in C_1 was <55% and for Ykc1-301 was 32%. (**C** and **D**) Similar to (A) and (B) except that the bath contained 20 mM instead of 100 mM K^+. The parameters for the Boltzmann fits in (D) were –51.0 mV, 22.3% and 100.0% for wild-type, –104.8 mV, 19.0% and 31.8% for *YKC1*-101, –93.3 mV, 12.22% and 8.3% for *YKC1*-301 and –92.7 mV, 16.9% and 32.9% for *YKC1*-402. Symbols are: wild-type, ○; Ykc1-101, □; Ykc1-301, △; Ykc1-402, ▽. The 0 time and steady-state current levels for (B) and (D) were determined from curve fits of the raw data (A and B) extrapolated to 0 and ∞ time respectively. Recording solutions and oocyte preparation were as described in Figure 1A. The stated holding potentials were held for at least 20 s prior to depolarization to +80 mV. Calibration bars 10 μA×100 ms.

Attempts were made to quantify residence in these closed states, but were thwarted by channel run-down over the course of the extended depolarization of excised patches.

PP mutations slow entry into the C_1 states

In addition to activation, entry into the delayed C_1 states was also examined. Twenty percent of the outward current resulted from activation from the delayed C_1 states when *YKC1*$^+$-expressing oocytes were stepped from 0 to +80 mV (100 mM bath K^+) (Figure 8A, uppermost trace of *YKC1*$^+$ traces; Figure 8B, ●, t = 0). Inward currents were not observed during a brief intervening step from 0 to –100 mV, yet still only 20% of the outward current was activated with delayed kinetics upon depolarization if the dwell at –100 mV was brief. Thus Ykc1 first enters C_2, not the delayed C_1 states, initially upon polarization to –100 mV. If the length of the –100 mV conditioning pulse was increased, an increasing fraction of the current was activated from the C_1 states (Figure 8A, *YKC1*$^+$, lower traces). When the fraction of the eventual steady-state current which was activated from the C_1 states was plotted against the dwell time at the –100mV conditioning pulse, it can be seen that all wild-type Ykc1 channels eventually migrated from the C_2 to the C_1 states at a combined rate of 280 and 2700 ms at –100 mV (Figure 8B, ●).

A similar voltage protocol was applied to oocytes expressing Ykc1-101 channels (Figure 8A, *YKC1*-101).

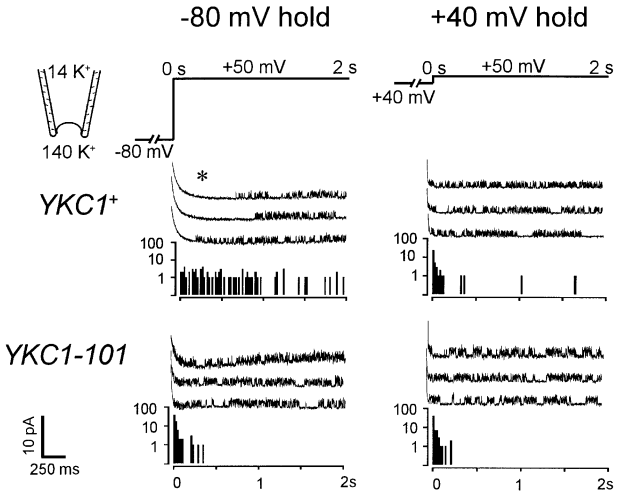

Fig. 7. Single channel analysis of emergence from the C_1 states. Latency analysis was conducted on $Ykc1^+$ (upper traces) and Ykc1-101 (lower traces). Excised inside-out single channel patches were held at either –80 (left) or +40 mV (right) for 10 s before stepping to the test potential of +50 mV. The latency to the first opening event at +50 mV was plotted on logarithmic event histograms below three representative traces shown for each condition. These histograms are each a compilation of at least 50 such measurements from patches from at least three separate oocytes. Bath (cytoplasmic) solutions contained 140 mM KCl and 5 mM EGTA. Pipette (external) solutions contained 14 mM KCl, 126 mM NaCl. Both solutions also contained 1 mM $CaCl_2$, 1 mM $MgCl_2$ and 5 mM HEPES, pH 7.2. Calibration bar 10 pA×250 ms.

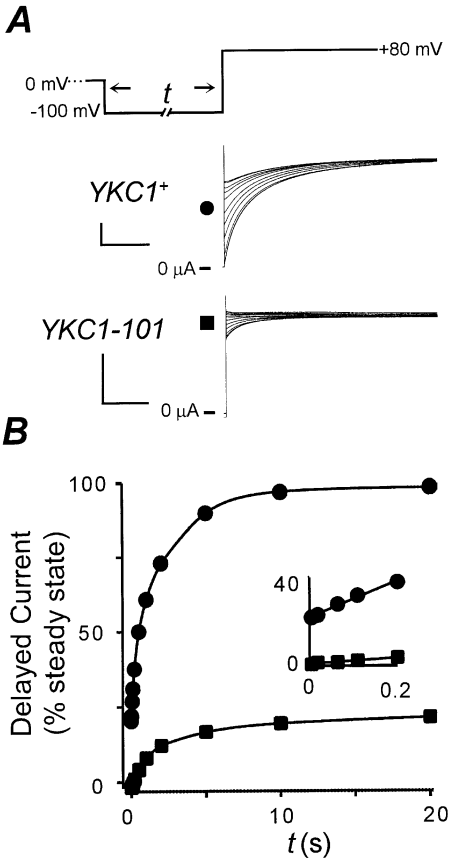

Fig. 8. PP mutation decreases $C_2 \rightarrow C_1$ transition rate. (**A**) Oocytes expressing either *YKC1*$^+$ (●) or *YKC1*-101 (■) RNA were repeatedly stepped to +80 mV in 100 mM bath K^+ from a holding potential of 0 mV with increasing intervening conditioning pulses at –100 mV. Traces show currents, from top, activating from conditioning pulses lasting 0, 10, 20, 50, 100, 200 and 500 ms and 1, 2, 5, 10 and 20 s. (**B**) The fraction of current activating with delayed kinetics, calculated as in Figure 6B, is plotted as a function of dwell time at the –100 mV conditioning pulse. Wild-type channels migrated from the C_2 to the slowly activating C_1 states at an initial rate at least eight times faster than Ykc1-101 channels (inset to B). Recording conditions and calculations were as described in Figure 6. Calibration bars 10 μA×200 ms.

Unlike the wild-type, only a minority of the mutant channels dwelt in the delayed C_1 states at steady-state at –100 mV. Because of this, the initial rate of $C_2 \rightarrow C_1$ transition was determined, so that any reverse $C_1 \rightarrow C_2$ transition of the mutant could be ignored. The inset of Figure 8B shows that the $C_2 \rightarrow C_1$ transition of the mutant channel was initially eight times slower than that of the wild-type. Thus, the Ykc1-101 PP mutation dramatically slows the transition from C_2 to the delayed C_1 states upon hyperpolarization.

Discussion

The findings presented in this report have several-fold significance. We have demonstrated that classical microbial selection can be fruitfully applied to structure–function studies of ion channels. Using microbial selection we have isolated Ykc1 mutants of functional consequence via their ability to block yeast proliferation. Despite the possibility of isolating a plethora of functional defects using such a general screen, only mutants which were defective in a single property, delayed C_1 states gating, were isolated under the conditions and criteria used in this study. By repeatedly and exclusively isolating mutations in the PP region, we have shown that this region plays a particularly important role in Ykc1 gating. By showing that other channel properties, such as ionic filtration and the C_2–O distribution, remain largely unaffected, we have shown that C_1 gating is determined, at least in part, by a domain of Ykc1 which is discrete from those which determine these other functions. Lastly, we may have uncovered evidence for a conserved gating function for the PP region among V and CNG cation channels.

PP mutations affect Ykc1 gating

At membrane potentials below E_K, *YKC1* dwells either in C_2, from which it can be activated near instantaneously, or C_1, from which it is activated slowly. We have found that rapid activation from C_2 to O is not a typical gating transition and thus we refer to C_2 and O as 'forms' of a single O/C_2 state (the wild-type C_2 properties are beyond the focus of the PP mutant analysis presented here and will be considered in a separate report; Loukin *et al.*, in preparation). The O/C_2 state remained intact in the PP mutants. Unitary conductance and ionic selectivity were unaffected (Figure 5). The activation rate from the rapid C_2 form was similar to that of the wild-type (Figure 4). The delayed C_1 states, in contrast, were substantially affected by the PP mutations. Far fewer mutant channels dwelt in the delayed C_1 states at potentials below E_K than did wild-type channels, which remain in the rapid C_2 form. The diminished distribution in the delayed C_1 states could be due either to a decrease in the stability of the delayed C_1 states relative to the C_2/O state or a defect in responding to the factors which drive Ykc1 to the delayed C_1 states (i.e. a defect in the sensor).

It is unlikely that the reduced distribution in the C_2 state is due to a defect in a sensor. The distribution between C_1 and C_2 at holding potentials below E_K (where no channels are in the conducting O form) appears to be determined by $\Delta\mu_{K+}$ (i.e. offset from E_K; compare Figure 6B with D). $\Delta\mu_{K+}$ also determines the steady-state rectification of Ykc1 (Figure 3). This rectification remains intact in the mutants and thus these mutants clearly have a normally functioning '$\Delta\mu_{K+}$ sensor' *per se*. A defective sensor causing the PP mutant phenotype would imply the existence of an additional $\Delta\mu_{K+}$ sensor. Having two independent $\Delta\mu_{K+}$ sensors within Ykc1 seems inordinately complex and we prefer a much simpler model in which residence in the C_1 states is a result of prolonged, uninterrupted residence in C_2 (the relationship between the wild-type C_1 and O/C_2 states will be discussed in detail elsewhere; Loukin *et al.*, in preparation)

The remaining possibility, destabilization of the delayed C_1 states relative to the C_2/O state, is the most attractive explanation for the decreased residence in the C_1 states by the PP mutant channels. That the activation rates from (Figure 6A) and the entry rates into (Figure 8B, inset) the C_1 states were altered by PP mutation further supports this conclusion. Although it cannot be determined here whether the PP region is the 'gate' of Ykc1, i.e. the region of the protein which actually occludes the deactivated channel pore, it can be concluded that the PP region is particularly important in determining stability of the closed

C_1 conformation relative to the O/C_2 conformation. Thus the PP region appears to be important in the gating of Ykc1. There is evidence that the PP region is the receptor for a 'ball-and-chain' type inactivating particle in Na^+ channels (McPhee *et al.*, 1995). It is unlikely that the PP region functions as such in Ykc1, since mutations in the 'ball' domain itself should have been isolated here.

C_1 states gating may not be exclusively determined by the PP region

The six growth blocking Ykc1 alleles isolated all occur in the PP regions of Ykc1: two residues in the first PP region, T322 and S330, and a single residue in the second PP region, V456. All six mutations occur within a 10 amino acid window relative to the aligned P regions (Figure 2B). Even if this window is doubled to 20 amino acids, the chance of this happening randomly is <1 in 1 000 000. Multiple independent isolations of the T322I and S330F mutations indicate that the screen is near saturation and therefore few other mutable residues are expected to cause growth blockage. There are, though, two caveats which prevent the conclusion that the PP domain is the only region which is involved in C_1 states gating.

The first is that the screening criteria used, complete blockage of proliferation, may preclude isolation of less severe C_1 states mutants. It is unlikely that more severe C_1 states mutants would not have been isolated, since Ykc1-301, which almost completely lacks functioning C_1 states (Figure 7B), was recovered. The second caveat is that the mutagen used, HA, primarily causes GC→TA transitions. This results in 42.5% of the amino acids of Ykc1 being immutable and limits the range of substitutions among the HA-mutable amino acids. This does not mean that 42.5% of the Ykc1 protein was not surveyed. We presume that functional domains of Ykc1 comprise multiple, not single, amino acids. Assuming a random distribution of immutable sites, the probability of a functional domain being HA-immutable should be 0.43^n, where n is the number of amino acids required for function of the domain. Although these caveats do not weaken the conclusion that the PP region is clearly important in C_1 states gating, they do raise the possibility that other regions are also potentially involved. It is clear, however, that the random mutagenesis employed here facilitates a much more comprehensive survey of the Ykc1 protein than a targeted approach would have.

Evidence of conserved gating function in the PP region

There is evidence for conserved gating function in the PP region among V and CNG cation channels. Whereas binding sites on the exterior side of the pore are accessible to externally applied TEA regardless of whether the channel is open or closed, binding sites on the cytoplasmic side of the channel pore are accessible to internally applied TEA only when the channel is in an open state (Armstrong, 1971; Stanfield, 1983), placing the channel gate on the cytoplasmic side of the channel pore. Gordon and Zagotta (1995) found that the binding of Ni^{2+} to histidine residues in the PP region of CNG channels affected gating, destabilizing the open state of olfactory CNG channels and stabilizing the open state of photoreceptor CNG channels relative to the closed state. Recently Liu *et al.* (1997) presented evidence for residues on the cytoplasmic side of M6 of the *Drosophilla* Shaker K^+ channel being intimately involved with gating of that channel. Given the extensive phylogenic divergence between fungi, insects and mammals, our results may suggest the existence of a conserved primordial gating function for the PP region of V and CNG cation channels.

Whereas comprehensive conservation of topological structure is clear among V and CNG channels, no comprehensive conservation of primary amino acid sequence is apparent. Conservation of structure and function in lieu of primary amino acid sequence conservation has been observed among other types of proteins, such as heme-containing globins, which have similar crystal structures yet sometimes bear no obvious primary sequence homology (Creighton, 1993). It is certainly tenable that intrinsic gating could be one of the functions driving the topological conservation among V and CNG channels.

Microbial selection in future studies of ion channels

In this report we have used yeast as a tool to show us which HA-mutable residues of Ykc1 are important in affecting those functions which block proliferation when incorrectly regulated. Here we focused on drawing correlations between the structural and electrophysiological properties of the Ykc1 molecule. The basis of growth blockage and the cell physiological role of wild-type Ykc1 are important and are being investigated (C.L.Fairman, X.-L.Zhou, R.Hoffman and C.Kung, in preparation).

We have shown that microbial selection of non-targeted mutants is indeed a powerful tool for correlating such functions preserved in domain structure but not obviously so in amino acid sequence. Without the guidance of conserved sequence, choosing appropriate residues to site specifically mutate is difficult. A second advantage of selecting randomly generated mutants is that the entire molecule is easily surveyed. By tailoring the screening method employed, looking for mutations which cause less severe disruption of growth or those which induce sensitivity to growth under particular ionic conditions, it should be possible to isolate mutants which induce subtler alterations of the C_1 states or other conserved functions of Ykc1.

Materials and methods

Strains and media

The budding yeast *S.cerevisiae* strain αku8 (MAT**a**, *leu2*-3/*112*, *ura3-1*, *trp1-1*, *ade2-1*, *his3-11/15*, *can1-100*, *ykc1*-Δ::*ura3*$^-$), which was exclusively used in these experiments, has been described previously (Zhou *et al.*, 1995). Cells were cultured either in standard rich yeast growth medium YEPD (Sherman, 1991), standard defined medium containing glucose as a carbon source (SD; Sherman, 1991) or SG, in which the glucose in SD was replaced by an equal weight of galactose.

Mutagenesis and mutant isolation

Mutant alleles of *YKC1* were generated by mutagenizing the plasmid pGALYKC1 (Zhou *et al.*, 1995) *in vitro* with HA by the methods described by Lee *et al.* (1995). The extent of mutagenesis was monitored by transforming mutated plasmids into a *pyrf* Amp^s bacterial strain (MH1066) which relies on the plasmid-borne *URA3* gene product for growth in the absence of exogenous uracil (Sikorski and Boeke, 1991). Two percent of the colonies were Ura$^-$, amp$^+$, indicating the loss-of-function mutation rate of the plasmid *URA3* gene, which is approximately

half the size of *YKC1*. Three separate pools of mutagenized plasmids were amplified in *Escherichia coli* and transformed into αku8 yeast using standard methods (Grey and Brendel, 1992; Ausubel *et al.*, 1993). Transformants were allowed to form colonies on uracil-deficient SD plates and these colonies were replica plated onto uracil-deficient SG to induce mutagenized *YKC1* expression. Colonies which failed to proliferate on SG were isolated from the original SD plate and rescreened for co-segregation of galactose sensitivity with the plasmid-borne Ura^+ phenotype (Ausubel *et al.*, 1993). Twenty two such mutants were isolated, 14 of which showed no growth and eight of which showed slow growth on SG. The mutagenized plasmids were recovered from all these strains. One or two plasmids which caused the no-growth phenotype were chosen from each of the four separately mutagenized pools to be analyzed further.

DNA sequence determination

Both strands of each allele of *YKC1* were sequenced using an ABI Prism Automated Sequencing kit and ABI 377 automated sequencer (Perkin Elmer). Five regularly spaced sequencing primers were used for each DNA strand. Sequencing templates were prepared using a plasmid miniprep kit (Qiagen).

Oocyte expression

The various *YKC1* alleles were excised from plasmid pGALYKC1 using *Bam*HI and *Hin*dIII, (Zhou *et al.*, 1995) and spliced into similar sites of the oocyte expression plasmid pGH19, resulting in precise insertion of the ORFs between the 5′- and 3′-untranslated regions (UTRs) of the *Xenopus* β-globulin gene and downstream of a T7 RNA polymerase promotor (pGH19 is a modification of the vector pGEMHE; Liman *et al.*, 1992). These constructs, termed pGHxxx, where xxx corresponds to the *YKC1* allele number (see text), were linearized downstream of the 3′-UTR of pGH19 to be used as templates in an *in vitro* T7 RNA polymerase reaction (mMessage mMachine, Ambion). For single channel experiments, ~0.5 ng RNA were injected and for two electrode voltage clamp experiments between 20 and 100 ng RNA were injected (100 ng for analysis of the rapid $C_2 \rightarrow O$ activation in Figure 4) into stage V and VI *Xenopus* oocytes. Frogs were maintained and oocytes were isolated and prepared as described in Goldin (1992) and Goldin and Sumikawa (1992).

Two electrode voltage clamp

One to four days after injection, currents were recorded from oocytes using a two electrode voltage clamp. A Geneclamp500 amplifier using HS-2A headstages and a VG-2A virtual ground bath clamp and pCLAMP 6.0 data acquisition software (all Axon Instruments) were used. To minimize serial resistance, 3 M KCl-containing current injection electrodes were used which had ~15 μm bores back-filled with a 2 M KCl, 2% agarose solution to prevent flow of KCl into the oocytes (Schreibmayer *et al.*, 1994). Data were filtered at 1 kHz at the point of acquisition without capacitive neutralization or leak subtraction. For recording rapid activation from the C_2 form (Figure 4), pipettes with bores of ~25 μm were used, data were filtered at 50 kHz, amplifier gain was set at its maximal level and stabilization was set to the minimal level which prevented 'ringing' (generally a phase lag of $\leqslant$20 μs). During all two electrode voltage clamp recording, V_m was simultaneously measured from the non-current-injecting electrode to verify that it reached the specified command potential.

Patch–clamp recording

For patch–clamp recording, the vitelline membrane was removed. This was achieved by a modification of standard protocols (Goldin and Sumikawa, 1992), squeezing and rolling oocytes with upwardly bent forceps in fresh Petri plates (which adhere to the membrane) containing 200 mM potassium glutamate, 20 mM KCl, 1 mM $MgCl_2$, 5 mM EGTA, 10 mM HEPES, pH 7.4, until the membrane ruptured and the devitellinized oocyte squeezed out. Currents were recorded using an EPC7 patch–clamp amplifier (List Medical Systems), filtered with a Bessel 8-pole filter at 1 kHz, digitized at 10 kHz and analyzed using pCLAMP 5.0 software (Axon Instruments). Unitary slope conductance was calculated from a linear regression of the apparent single open channel conductance measured at +10, +20, +30, +40 and +50 mV. These unitary conductances were measured as the distance between peaks of amplitude histograms of single channel inside-out patches in the presence of 140 mM bath and 14 mM pipette K^+.

Acknowledgements

We thank G.A.Robertson for providing *Xenopus* oocytes, T.Miosga for providing yeast strains, P.Blount for critical reading of the manuscript and R.Hoffman for technical assistance. S.L. is a trainee in the DEO/NSF/USDA Collaborative Program on Research in Plant Biology. This work was partially supported by NIH grants GM 22714 and 36386.

References

Armstrong,C.M. (1971) Interaction of tetraethylammonium ion derivatives with the potassium channels of giant axons. *J. Gen. Physiol.*, **58**, 413–437.

Ausubel,F.M., Brent,R., Kingston,R.E., Moore,D.M., Seidman,J.G., Smith,J.A. and Struhl,K.A. (1993) *Current Protocols in Molecular Biology.* Greene Publishing Associates and John Wiley-Interscience, New York.

Bertl,A., Slayman,C.L. and Gradmann,D. (1993) Gating and conductance in an outward-rectifying K^+ channel from the plasma membrane of *Saccharomyces cerevisiae. J. Membr. Biol.*, **132**, 183–199.

Bertl,A., Anderson,J.A., Slayman,C.L. and Gaber,R.F. (1995) Use of *Saccharomyces cerevisiae* for patch–clamp analysis of heterologous membrane proteins: characterization of Kat1, an inward-rectifying K^+ channel from *Arabidopsis thaliana*, and comparison with endogeneous yeast channels and carriers. *Proc. Natl Acad. Sci. USA*, **92**, 2701–2705.

Creighton,T.E. (1993) *Proteins: Structures and Molecular Properties.* 2nd Edn. W.H.Freeman and Co., New York.

Czempinski,K., Zimmermann,T.E., Ehrhardt,T. and Müller-Röber,B. (1997) New structure and function in plant K^+ channels: KCO1, an outward rectifier with a steep Ca^{2+} dependency. *EMBO J.*, **16**, 2565–2575.

Fink,M., Duprat,F., Lesage,F., Reyes,R., Romey,G., Heurteaux,C. and Lazdunski,M. (1996) Cloning, functional expression and brain localization of a novel unconventional outward rectifier K^+ channel. *EMBO J.*, **15**, 6854–6862.

Goldin,A.L. (1992) Maintenance of *Xenopus laevis* and oocyte injection. *Methods Enzymol.*, **207**, 266–278.

Goldin,A.L. and Sumikawa,K. (1992) Preparation of RNA for injection into *Xenopus* oocytes. *Methods Enzymol.*, **207**, 279–298.

Goldstein,S.A., Price,L.A., Rosenthal,D.N. and Pausch,M.H. (1996) ORK1, a potassium-selective leak channel with two pore domains cloned from *Drosophila melanogaster* by expression in *Saccharomyces cerevisiae*. *Proc. Natl Acad. Sci. USA*, **93**, 13256–13261.

Gordon,S.E. and Zagotta,W.N. (1995) A histidine residue associated with the gate of the cyclic nucleotide-activated channels in rod photoreceptors. *Neuron*, **14**, 177–183.

Grey,M. and Brendel,M. (1992) A ten-minute protocol for transforming *Saccharomyces cerevisiae* by electroporation. *Curr. Genet.*, **22**, 335–336.

Gustin,M.C., Martinac,B., Saimi,Y., Culbertson,M.R. and Kung,C. (1986) Ion channels in yeast. *Science*, **233**, 1195–1197.

Gustin,M.C., Zhou,X.L., Martinac,B. and Kung,C. (1988) A mechanosensitive ion channel in the yeast plasma membrane. *Science*, **242**, 762–765.

Ketchum,K.A., Joiner,W.J., Sellers,A.J., Kaczmarek,L.K. and Goldstein, S.A. (1995) A new family of outwardly rectifying potassium channel proteins with two pore domains in tandem. *Nature*, **376**, 690–695.

Lee,H.C., Toung,Y.P., Tu,Y.S. and Tu,C.P. (1995) A molecular genetic approach for the identification of essential residues in human glutathione S-transferase function in *Escherichia coli*. *J. Biol. Chem.*, **270**, 99–109.

Lesage,F., Guillemare,E., Fink,M., Duprat,F., Lazdunski,M., Romey,G. and Barhanin,J. (1996) A pH-sensitive yeast outward rectifier K^+ channel with two pore domains and novel gating properties. *J. Biol. Chem.*, **271**, 4183–4187.

Lesage,F., Lauritzen,I., Duprat,F., Reyes,R., Fink,M., Heurteaux,C. and Lazdunski,M. (1997) The structure, function and distribution of the mouse TWIK-1 K^+ channel. *FEBS Lett.*, **402**, 28–32.

Liman,E.R., Tytgat,J. and Hess,P. (1992) Subunit stoichiometry of a mammalian K^+ channel determined by construction of multimeric cDNAs. *Neuron*, **9**, 861–871.

Liu,Y.M., Holmgren,M.E., Jurman,M.E. and Yellen,G. (1997) Gated access to the pore of a voltage-dependent K^+ channel. *Neuron*, **16**, 859–867.

McPhee,J.C., Ragsdale,D.S., Scheuer,T. and Catterall,W.A. (1995) A critical role for transmembrane segment IVS6 of the sodium channel alpha subunit in fast inactivation. *J. Biol. Chem.*, **270**, 12025–12034.

Miosga,T., Witzel,A. and Zimmermann,F.K. (1994) Sequence and function analysis of a 9.46 kb fragment of *Saccharomyces cerevisiae* chromosome X. *Yeast*, **10**, 965–973.

Reid,J.D., Lukas,W., Shafaatian,R., Bertl,A., Scheurmann-Kettner,C., Guy,H.R. and North,R.A. (1996) The *S. cerevisiae* outwardly-rectifying potassium channel (DUK1) identifies a new family of channels with duplicated pore domains. *Receptors Channels*, **4**, 51–62.

Schreibmayer,W., Lester,H.A. and Dascal,N. (1994) Voltage clamping of *Xenopus laevis* oocytes utilizing agarose-cushion electrodes. *Pflugers Arch. Physiol*., **426**, 453–458.

Sherman,F. (1991) Getting started with yeast. In Guthrie,C. and Fink,G.R. (eds), *Guide to Yeast Genetics and Molecular Biology.* Harcourt Brace Jovanovich, San Diego, CA, Vol. 194, pp. 3–21.

Sikorski,R.S. and Boeke,J.D. (1991) *In vitro* mutagenesis and plasmid shuffling: from cloned gene to mutant yeast. In Guthrie,C. and Fink,G.R. (eds), *Guide to Yeast Genetics and Molecular Biology.* Harcourt Brace Jovanovich, San Diego, CA, Vol. 194, pp. 302–318.

Stanfield,P.R. (1983) Tetraethylammonium ions and the potassium permeability of excitable cells. *Rev. Physiol. Biochem. Pharmacol*., **97**, 1–67.

Zhou,X.L., Vaillant,B., Loukin,S.H., Kung,C. and Saimi,Y. (1995) *YKC1* encodes the depolarization-activated K^+ channel in the plasma membrane of yeast. *FEBS Lett*., **373**, 170–176.

Received on April 24, 1997; revised on June 5, 1997